Molecular Crystals and Liquid Crystals
Publication details, including instructions for authors and subscription information:
http://www.informaworld.com/smpp/title~content=t713644168

Light Controlled Capillarity of Liquid Crystals on Photo Anisotropic Surfaces

Guillaume Goubert[a]; Tigran V. Galstian[a]
[a] Center for Optics, Photonics and Laser, Department of Physics, Engineering Physics and Optics, Laval University, Québec, Canada

First published on: 19 August 2010

To cite this Article Goubert, Guillaume and Galstian, Tigran V.(2010) 'Light Controlled Capillarity of Liquid Crystals on Photo Anisotropic Surfaces', Molecular Crystals and Liquid Crystals, 526: 1, 46 — 57
To link to this Article: DOI: 10.1080/15421406.2010.485068
URL: http://dx.doi.org/10.1080/15421406.2010.485068

Mol. Cryst. Liq. Cryst., Vol. 526: pp. 46–57, 2010

ISSN: 1542-1406 print/1563-5287 online
DOI: 10.1080/15421406.2010.485068

Taylor & Francis
Taylor & Francis Group

Light Controlled Capillarity of Liquid Crystals on Photo Anisotropic Surfaces

GUILLAUME GOUBERT AND TIGRAN V. GALSTIAN

Center for Optics, Photonics and Laser, Department of Physics, Engineering Physics and Optics, Laval University, Québec, Canada

We report the observation and experimental study of an anisotropic photo controlled capillarity effect in liquid crystal cells. The photo sensitive substrates of the cell are composed of reactive mesogen host that is doped by guest azobenzene dye. We first describe the study of photo induced phenomena in those substrates, then the capillary propagation of the liquid crystal that is blocked in the areas exposed to circularly polarized light. We believe that the wetting of the surface is changed by the photo induced molecular reorientation of the surface. In addition, this reorientation forces a corresponding reorientation of the liquid crystal during its penetration. The corresponding orientational deformation energy then changes the balance of forces and the corresponding capillary action.

Keywords Azo dye; capillarity; liquid crystals; photo induced anisotropy; reactive mesogens; wetting

Introduction

Capillarity represents important practical and fundamental interest [1]. As it is well known, the capillarity phenomena are predetermined by the wetting properties of the surface. However, various techniques may be used to change those properties. These modifications may have permanent chemical [2] or architectural character (such as the lotus flower [3]) or a dynamic (reversible) character. Known dynamic control mechanisms are the use of temperature [4], electric field [5,6] and light (see below).

An interesting type of photo controllable (reversible) wetting phenomena was reported in material systems containing azobenzene dye molecules, either doped into the wetting liquid or introduced on the solid surface. Thus, a dynamic UV control of the surface tension of liquid solutions was demonstrated, using light to change the extent of aggregation of surfactants within the bulk solution (by using water soluble surfactants that contain azobenzene [7]). In contrast, for a solid surface, which contains azobenzene molecules, a net mass transport was demonstrated by asymmetrical photo irradiation, which caused a gradient in surface free energy due to the photo isomerization of surface azobenzenes, leading to the directional motion of the droplet [8].

Address correspondence to Tigran V. Galstian, Center for Optics, Photonics and Laser, Department of Physics, Engineering Physics and Optics, Laval University, Pav. d'Optique-Photonique, 2375 rue de la Terrasse, Quebec, G1V OA6, Canada. Tel.: 418-656-2025; E-mail: galstian@phy.ulaval.ca

The above mentioned experiments have investigated azobenzene dye interactions with isotropic liquids only. The study of interaction of azobenzene containing surfaces with anisotropic liquids, such as liquid crystals (LC), was reported in several works [9,10] (see also the review in Ref. [11]). However, to the best of our knowledge, all those investigations focused on the optical control of the orientation of the director (average direction of long molecular axes [12]) of the LC and no observations were reported concerning the photo induced capillarity or wetting effects due to the photo anisotropic character of the liquid – surface interactions.

Recently we have reported the observation of optical control of capillary propagation of the LC into a cell the substrates of which contained azobenzene dyes [13]. In the present work we are reporting the further study of light induced reorientation of mesogenic molecules of the host layer having azobenzene dyes as guest and the resulting control of capillarity and wetting of nematic LCs. Detailed study of the composite substrates and of LC filling conditions confirm the anisotropy character of the phenomenon. In fact, the key feature of this phenomenon is the generation of an additional source of free energy, which is the energy of orientational deformation of the director of the LC, which affects the conditions of liquid's capillary propagation.

Material System and Substrate

We used a commercially available reactive mesogen (RM) material RMS03-001C (from Merck) dissolvent in the solvent PGMEA (from Merck) for spin coating. The concentration of the RM in the PGMEA was 30 wt%. This RM was chosen for several reasons: firstly, this material is in the liquid crystalline mesophase at room temperature, which greatly facilitates experimental work (the Nematic-Isotropic phase transition is 70°C and the solution must be kept above 4°C to avoid crystallization). Also, we used this RM since it adopts a planar alignment when spin coated on a rubbed "planar" polyimide (PI) surface.

Before being spin coated on the PI, the mixture of RMS03-001C/PGMEA was doped (1 wt%) by the azobenzene dye (further called AZD2 [14]) as shown on Figure 1.

The mixture was homogenized using magnetic mixers and an ultrasound bath for 20 minutes. 1 wt% of PI (PI150), dissolved in the solvent S21 (both from Nissan Chemicals, LTD), was used to generate planar alignment (see later). The LC material used was the nematic mixture TL216 (from Merck). It has a positive optical anisotropy.

Commercially available (from TFD) indium tin oxide (ITO) coated float glass substrates were used to build "sandwich" cells. Those substrates (with sizes 10 mm × 10 mm × 0.7 mm) were first cleaned and then covered by a thin film of PI by spin coating. The spin coating conditions were: 500 rpm for 5 s, then 3000 rpm

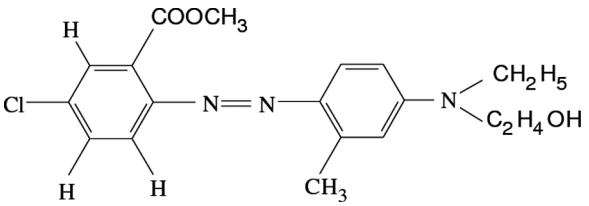

Figure 1. Schematic representation of the AZD2 molecular structure.

for 20 s. The PI coated ITO-glass substrates were then heated in an oven (80°C for 10 minutes, then 280°C for 60 minutes) to remove the rest of the solvent and to bake the PI prior to mechanical rubbing. After this step the PI layer was submitted to mechanical rubbing. The thickness of PI layer obtained was between 60–80 nm (as measured by a Dektak profile meter and a Horiba Jobin Yvon ellipsometer).

The final step of the substrate preparation was the spin coating of a thin layer of the AZD2 doped RMS03-001C/PGMEA solution, described above. The spin coating conditions were: 500 rpm for 5 s, then 3000 rpm for 20 s. The film was then prebaked at 56°C for 1 minute.

As already mentioned, at room temperature, the obtained layer was in the LC phase and was aligned in the direction of the PI's rubbing. This was first verified by using a standard polarimetric set-up. In addition, the further spectral studies of obtained films showed not only optical anisotropy, but also significant linear dichroism thanks to the natural alignment of AZD2 (which is a dichroic dye) along with the RM's alignment, see Figure 2. It is clear that the absorption is dominated by the *Trans* (rod like) form of the AZD2 and is higher for the parallel (with the rubbing direction) polarized probe, except the spectral area above 600 nm, where the long wavelength wing of the absorption of the *Cis* (less rod like) form of the AZD2 prevails [14].

Cell Fabrication

The obtained films of AZD2 doped RM were then polymerized to avoid their degradation in time or to prevent their dissolving into the LC when put in contact with. Thus, the glass substrate (coated with ITO/PI/RM film) was then inserted into a chamber with optical windows. The chamber was filled with Nitrogen (to minimize the access of Oxygen) and the RM layer was photo polymerized for 20 minutes by means of a spatially uniform non polarized UV light at normal incidence (UV lamp intensity was $\approx 5\,\mathrm{mWcm}^{-2}$ (measured with Gentec UV power meter) and its spectra was centered at 375 nm. The oriented and solidified RM layers, thus obtained, had thicknesses ranging from 600–800 nm (measured by profile meter and ellipsometer). Two such substrates were then used (with the RM layers facing each other) to build a LC cell of thickness $L = 50\,\mu\mathrm{m}$ (using spherical spacers mixed into a UV curable glue, which was dispensed on the periphery of the cell).

In contrast to the above mentioned procedure, another set of substrates was UV polymerized while being simultaneously exposed by a circularly polarized CW Ar+ laser beam (operating at 514.5 nm, near the absorption peak of the AZD2, Fig. 2). The diameter of the laser beam was $2\,\mathrm{mm} \pm 0.2\,\mathrm{mm}$ and its power was varied (for different experiments) between 50–150 mW. The laser beam was incident from air (at normal incidence) onto the RM layer to avoid the possible change of its polarization if it would be propagated in the RM layer (incidence from the glass side). This was done to reorient the AZD2 [15] and consequently the RM molecules [16] in the direction normal to the surface. As it can be seen, from the Figure 3, the absorption spectra of those exposed films are quite different from non-exposed ones (Fig. 2). Thus, the absorption of the parallel polarized probe is now significantly reduced (for the normally incident probe beam) while the perpendicular polarization component remains at the same order of magnitude. This is the result of the reorientation of AZD2 molecules in the direction of the normal of the surface (wave vector of the excitation beam [15]). We can also notice an increase of the *Cis* absorption (with inversed dichroism below 500 nm, which was already reported in Ref. [17]).

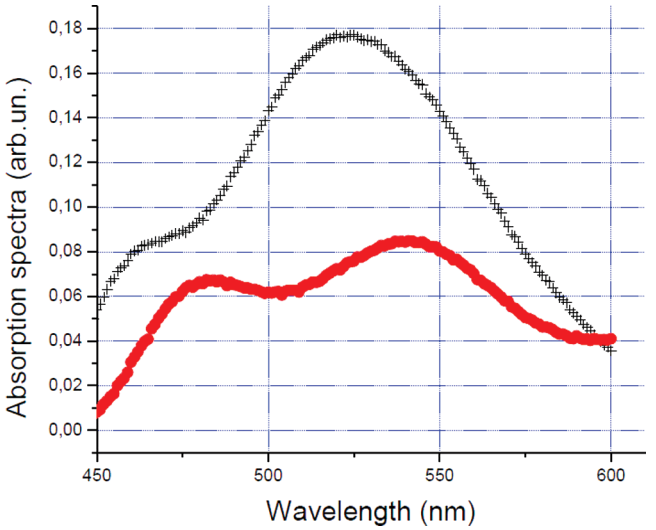

Figure 2. Absorption spectra of the original (non exposed) azobenzene dye doped reactive mesogene film that was spin coated on a rubbed polyimide. Crosses represent data for probe polarization that is parallel with the rubbing direction, while filled circles show the data for the perpendicular polarization.

The impact of the dye excitation and reorientation on the anisotropy of the film has been also studied by using a dynamic polarimetric set-up. Namely, the film (and the UV polymerization setup) was inserted between two crossed polarizers with its rubbing direction oriented at 45° with respect to the polarizer's axis. The linearly polarized probe beam (He-Ne laser operating at 632.8 nm) was traversing (at normal

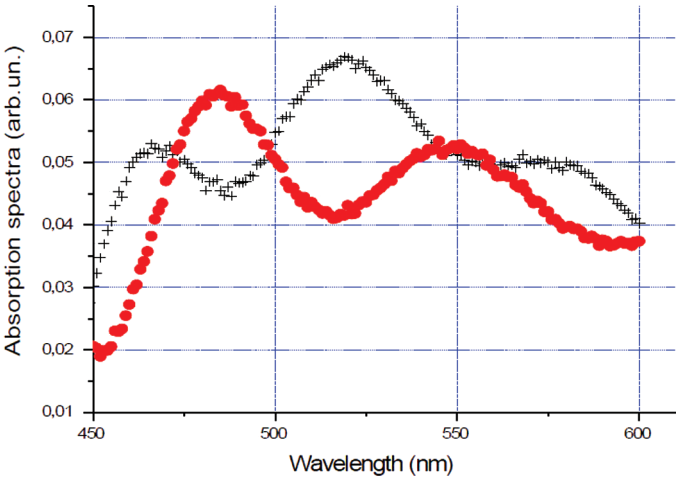

Figure 3. Absorption spectra of the circularly polarized laser exposed (at normal incidence) azobenzene dye doped reactive mesogene film that was spin coated on a rubbed polyimide. Crosses represent data for the probe polarization that is parallel with the rubbing direction, while filled circles show the data for the perpendicular polarization.

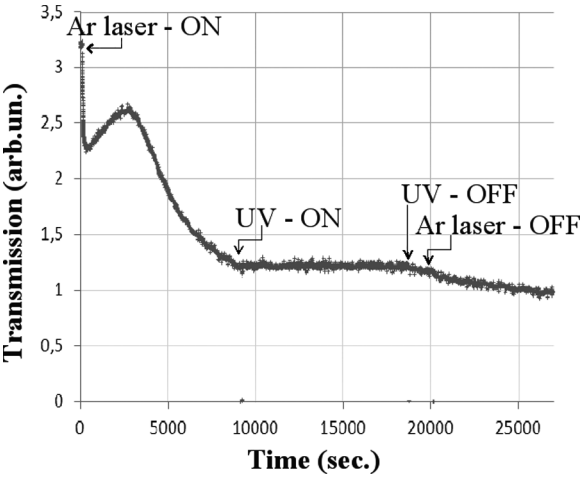

Figure 4. Polarimetric signal's dynamics. Different key stages of the experiment are identified on the graph.

incidence) the area that was exposed by the circularly polarized Ar laser beam (at nearly normal incidence). The dynamics of probe transmission through the analyzer is shown in the Figure 4. As we can see, the transmission is quickly reduced when the excitation beam is switched on. There is then a relatively slow growth followed by a faster decrease with further stabilization tendency. Adding the polymerizing UV lamp helps this stabilization and, when the UV and Ar light are both removed, the final transmission remains at a level that is quite different (lower) from the initial one. We believe that this curve again confirms the above mentioned hypothesis that the AZD2 is excited by the Ar laser from its *Trans* state to its *Cis* state, which is quickly destabilizing the orientational order (and thus the local anisotropy) of the RM and also is absorbing more the probe light [14]. The further slow increase of the signal should be related to the stabilization of the *Trans-Cis-Trans* transformation process along with a partial reestablishment of the local anisotropy value. However, the further continued (multiple cycles of) excitation of the dye and its orientational redistribution (alignment along the normal of the film) forces a corresponding reorientation of the RM molecules too, which brings to a reduced *in-plane* anisotropy of the film and thus to a reduced transmission through the analyzer. The addition of the UV light polymerizes the RM matrix, which reduces significantly the orientational (angular) mobility of all species, stabilizing thus the structure under excitation. The matrix is finally stabilized (with relatively small variations) once all excitation sources are removed.

Experimental Observations

The obtained substrates were used to build cells and the LC was introduced into the cell by capillary action at room temperature. Those cells had well aligned LC orientation in the areas which were not exposed to the laser beam during the UV photo polymerization (verified by the microscope and polarimetric set-up). In fact, those cells, which were fabricated without the laser exposed substrates, were filled in the standard way; uniform fill and orientation of the LC were obtained. In

contrast, those cells which were build by using laser exposed substrates, showed an extraordinary behavior. Namely, the capillary action moved the LC up to the laser exposed area as usual. However, this LC movement stopped near to the border of the area exposed to the laser light. The LC completed the fill process everywhere else, while an air bubble was formed in the area, which was exposed to the laser beam (Fig. 5). We wish to emphasize that, in contrast to occasional air bubbles that may time-to-time appear in capillary fill experiments, the air bubbles obtained in our case are always in the same position (in the laser exposed area), they have the same form, they do not move neither during nor after the capillary fill and they are extremely stable. Also, the diameter of the air bubble ($2.3\,\text{mm} \pm 0.2\,\text{mm}$) is approximately equal to the diameter of the laser beam. The same fill experiment, done at higher temperatures, for which the LC is in the isotropy phase, shows that the entire cell (including the laser exposed area) is filled by capillarity. This clearly demonstrates the anisotropy character of the phenomena observed.

Note that the surface analysis (made by means of a Quesant atomic force microscope, AFM) did not reveal any noticeable relief modulation in the area exposed by the laser. Also, both AFM and microscope analyses do not show any sign of phase separation in that area. This is why we think that the formation of the air bubble during the capillary fill is primarily related to the reorientation of surface molecules (both azo and RM).

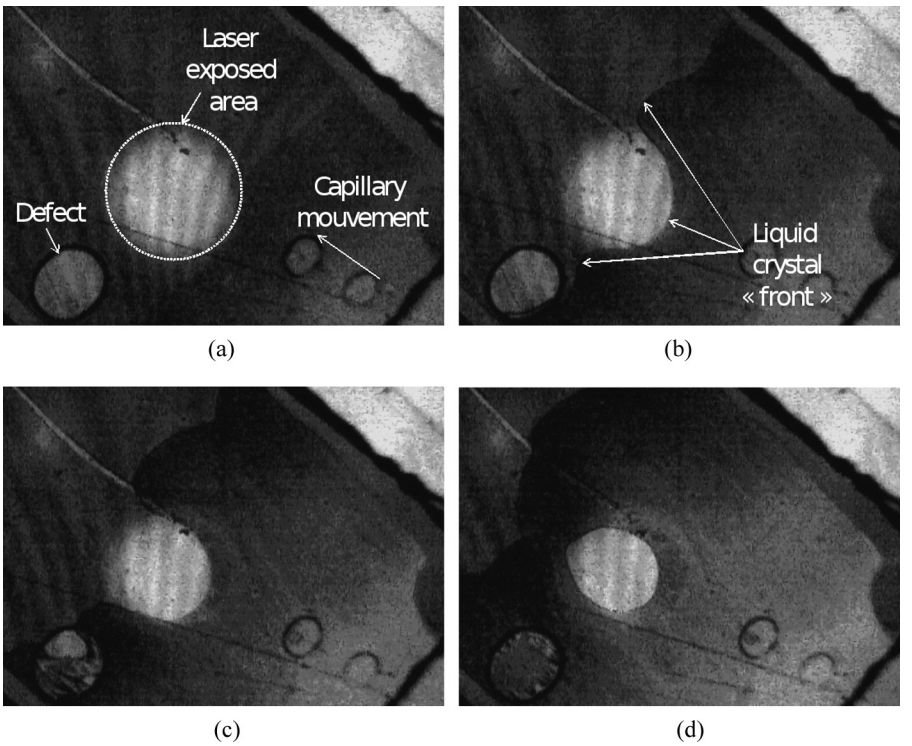

Figure 5. Microphotography of the capillarity movement of the liquid crystal into the cell with locally laser exposed substrates (the area shown by the dotted circle). Figures (a)–(d) refer on a sequence of photos showing the dynamic filling of the cell. Note that the left bottom and right bottom defects are filled by the LC while the central (laser exposed area) is not.

Closer analyses (done by using a polarizing microscope) of the ''wall'', which separates the air bubble from the LC, shows complex multiple zone structure that was already reported in the Ref. [13]. It must be noted that a special care was made to assemble the cell in such a way to have the laser exposed areas of two substrates exactly facing each other. In the case, if the adjustment of two substrates was not ideal (centers of exposed zones are not on the same axis) the obtained cell had different typical zones : first of all those are zones with non exposed planar uniform alignment on both substrates; then there are zones with hybrid alignment (vertical on the exposed substrate and planar on the non exposed substrate) and finally zones where the vertical alignment is promoted on both substrates (both exposed by laser). The Figure 6 shows such a misaligned situation. The assembled cell is placed between two crossed polarizers and illuminated by an expanded probe beam. Two black rings represent schematically the laser exposed zones on two substrates.

One can quantify the degree of variation (the gradient) of LC director (at ground state as well as under dielectric torque) by counting the number of ''interferential'' rings. Thus, the Figure 7 shows the number of rings counted along a line drawn from the center of exposition area to the periphery (see previous Fig.) for different voltages (square like wave form) applied to ITO electrodes. The excitation frequency is 1 kHz. As it can be seen, the number of rings starts changing already for 0.5 V (thanks to the director reorientation in the laser exposed zones where the pretilt is increased as a result of the laser exposition), while the Frederick's transition

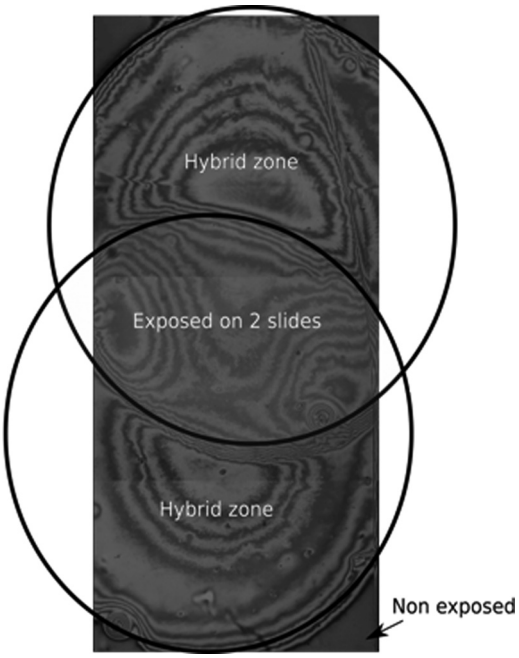

Figure 6. ''Interferential'' rings produced by the transmission of light through the LC cell (placed between crossed polarizers) with misaligned centers of laser exposed zones. Two black rings represent schematically the laser exposed zones on opposed substrates. The central part (where two rings overlap) corresponds to the zone where opposed sides of substrates where exposed by circularly polarized laser beams.

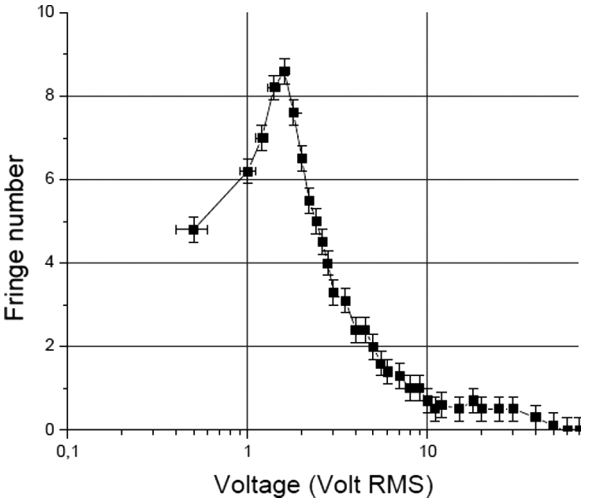

Figure 7. Dependence of the number of the rings (counted along a line from the center of laser exposed area to the periphery) upon the applied voltage. The maximum of fringe numbers corresponds to the Fredericks transition in the non exposed area.

(corresponding to the maximum number of rings) is achieved at the order of 1.1 V for the non exposed zones. With the further increase of the voltage all zones become homeotropically oriented reducing thus the number of rings. Note that the laser created pretilt (at the surface of the exposed area) may be estimated to be approximately $52^\circ \pm 4^\circ$ by counting the number of those rings in the approximation of uniform gradient of the director's angle in the direction of the normal of the cell.

Discussion

We believe that the observed phenomena are clearly defined by the light induced gradient of RM molecule alignment on the internal surfaces of the LC cell. Both polarimetric and spectral experiments show the creation of such molecular reorientation towards the normal of the substrates (resulted by the exposition of a normally incident circularly polarized light). Given the mesogenic character of the RM, this orientation is "imposed" to the LC when it propagates by capillarity in the cell. Thus, in addition to the traditional coupling [12] of the flow of the LC's velocity field with the director field, we obtain non uniform (in space) boundary condition affecting the orientational configuration of the director during the propagation. It seems thus that the laser exposition creates an energetic barrier for the capillary propagation of the LC near the periphery of the laser exposed area and reduces the further surface wetting by the LC. Let us emphasize, that in contrast to "traditional" mechanisms, this exposure did not change the chemical composition of the surface. In "traditional" liquid-solid systems, the contact angle θ is described by the Young's equation for flat and solid surfaces [1].

$$\gamma_{LV} \cos \theta = \gamma_{SV} - \gamma_{SL}$$

where γ_{SL}, γ_{SV}, and γ_{LV} are surface tensions (interfacial free energy per unit area) of the solid-liquid, solid-vapor and liquid-vapor interfaces, respectively.

As we have mentioned already, in our material system, the laser exposition may generate two phenomena: *Trans* to *Cis* photo isomerization of the AZD2 and reorientation of the *Trans* molecules (as a result of multiple cycles of *Cis* to *Trans* relaxation) into directions, where the dipole moments of those molecules have lower projections on the polarization of the excitation laser [14]. Thus, in the case of a circularly polarized and normally incident laser beam, this is the direction of the normal of the surface [15]. Given the liquid crystalline character of the host matrix (the RM), into which the AZD2 molecules are doped, the reorientation of azobenzene dyes should force the "collective" reorientation of the molecules of the RM too [18]. For the same reason (the liquid crystalline character of the RM) the molecules of the LC are later forced to follow the same reorientation. In fact, initially the RM aligns naturally in the rubbing direction of the PI. The same happens to the LC molecules when they are put in direct contact with the same PI surface. So it is quite natural that the LC is aligned in the planar direction on non exposed (to the circularly polarized laser) surfaces after the capillary fill. We believe that it is also natural that the orientation of the LC must undergo a strong deformation when approaching the laser exposed area, since in this area, the surface molecules are reoriented to be perpendicular to the surface as a result of the simultaneous exposure to circularly polarized light and UV polymerization.

The schematic representation of such capillary fill may be found in the Figure 8 (the cross section of the cell). The arrow (from left to right) shows the propagation direction of the LC. Figure 8a shows the LC propagation process in the non exposed (by laser) area in the case where the air-LC interface is homeotropic (LC molecules are aligned perpendicular to the air-LC surface). Since the alignment of surface molecules (both AZD2 and RM) is planar, then the capillary action should create two disclination lines near to the top and bottom corners of the propagation front (shown by two dots). Still in the case of homeotropic air-LC interface, the situation changes when the LC approaches the laser exposed areas, as demonstrated by the vertical dotted line in the Figure 8b. As demonstrated schematically, in this area, the perpendicular orientation of surface molecules should reduce the elastic deformation energy, helping thus to keep the wetting angle low and promoting good propagation due to capillary. In contrast, in the case of planar air-LC interface (LC molecules are parallel to the air-LC surface), the initial orientational deformation energy (with only one disclination line when propagating in non exposed areas, Fig. 8c) increases when the LC approaches the laser exposed area (Fig. 8d). This laser exposed area is shown extending from the line 3 and to the right of the line 1. One can see schematically that the further propagation of LC in those areas is possible "at the price" of the formation of two additional disclination lines (shown by two dots). Thus, those areas create an energetic barrier for the capillary propagation. We must emphasize that, in general, the alignment at air-LC interface may be different for different LC compositions.

The previously mentioned zones of the "air-bubble" walls are schematically positioned (in a very approximate way) in the Figure 8d by vertical dotted lines 1–3. The area on the left side of the vertical line 3 is the uniform (planar) oriented LC. The area between lines 3 and 2 is the orientational transition zone. The area on the right side of the line 1 is the air bubble. The electro-optical "movements" of the three "walls" (reported in Ref. [13]) under the action of the electric field are thus related to the fact that the liquid crystal has a positive dielectric anisotropy and is forced to align parallel with the applied electric field. However, it is well known [19,20] that the air-LC interface has a very strong energy and may be considered as

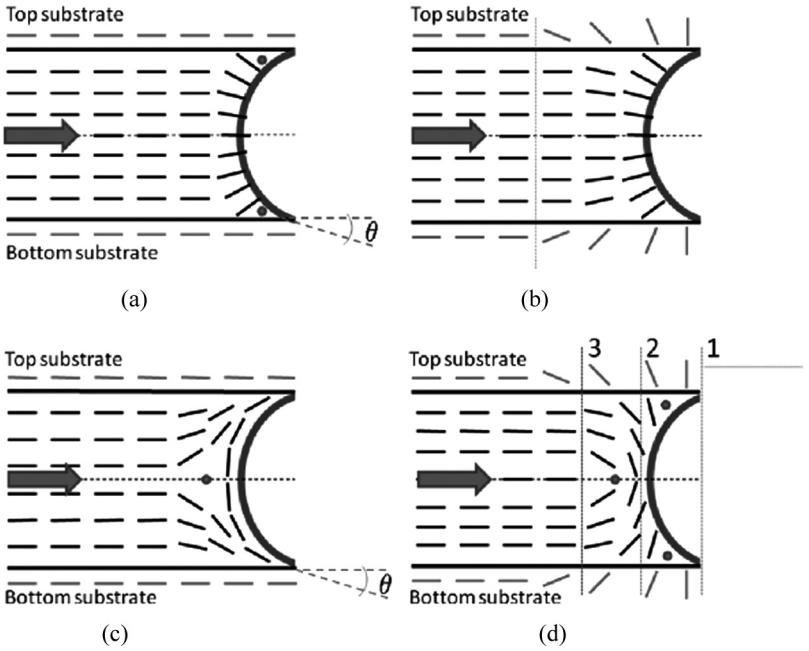

Figure 8. Schematic (cross section) representation of the capillary fill process of the liquid crystal in the cases of (a)&(b) homeotropic alignment of molecules at air-LC interface and (c)&(d) planar alignment of molecules at air-LC interface. (a)&(c) show the capillary propagation in uniform (non-exposed) areas, while the (b)&(d) show the capillary propagation near to the laser exposed areas. The dashed lines inside of the two parallel (horizontal) solid lines represent the LC molecules. The dashed lines outside of the two parallel (horizontal) solid lines represent the molecules of reactive mesogene and azo dye. The arrow shows the LC flow direction (from left to right). The area on the right side of the curved surface is the air bubble. θ is the wetting angle. Dots represent the disclination lines. Laser exposed area is on the right side of the vertical line 3.

strongly oriented layer. That is why there is a narrow zone (delimited by the line 2) near the air-LC interface which is affected much less. Similarly, the extreme limit of that zone (delimited by the line 1) is affected very weakly. Thus, the movements of the lines 1&2 are related to the change of molecular orientation of the near surface (air-LC) zone and of the LC wetting angle.

To recapitulate, we obtain a solid surface, the chemical composition of which is uniform and which must be wet to allow the LC propagation. However, the molecular orientation of this surface is not uniform. When approaching the laser exposed zone, the LC molecules tend to be oriented in the direction of RM/AZD2 molecules (along the normal of the surface) given their liquid crystalline character. This creates additional free energy (due to the additional orientational deformation of LC, see below) and prohibits the capillary fill. The application of an electric field causes the reorientation of LC molecules and moves the border 3 towards the center of the air bubble. This reorientation is significantly less for border 2 since there is already a bend reorientation (towards the normal of the surface) of LC molecules and the border is too close to the air-LC interface. The movement of border 1 is rather small too and is related to the movement of the internal wall of LC and its wetting angle.

If we suppose that, in the static regime, there is, for example, a bend deformation of the director $\vec{n}$, then the corresponding (to that deformation) additional volume free energy density F_d of the nematic LC may be expressed by the equation $F_d = \frac{1}{2}K_3(\vec{n} \times r\vec{o}t(\vec{n}))^2$, where K_3 is the corresponding elastic constant (typically at the order of 10^{-6} erg/cm) [12,21]. For a deformation scale of l, and in the so called one-constant elasticity approximation ($K_1 = K_2 = K_3 \equiv K$), the very rough estimation of the energy F_d may be evaluated by the following expression $F_d \approx \frac{K}{l^2}$ [12,21]. Thus, for a typical value of $l \approx 0.2 \cdot 10^{-3}$ cm (the typical size of the "movement" of the line 2, at the order of 2 μm) we obtain $F_d \approx 25\,\mathrm{erg} \cdot \mathrm{cm}^{-3} = 2.5\,\mathrm{N} \cdot \mathrm{m}^{-2}$. At the same time the surface tension coefficient A (which is at the order of U_{NS}/a^2; where U_{NS} is the anisotropic part of the energy of Nematic-Substrate interaction and a is the average molecular length) may be estimated as $A \approx 0.5K_3L^2q^3$, where $q = 2\left(\frac{\pi}{l}\right)$) [12,21]. We obtain (by using the values $l \approx 0.2 \cdot 10^{-3}$ cm; and thus $q = 31.4 \cdot 10^3\,\mathrm{cm}^{-1}$) the order of magnitude of

$$A \approx 0.5 \cdot 10^{-6}\,\mathrm{erg} \cdot \mathrm{cm}^{-1} \cdot 2025 \cdot 10^{-8}\,\mathrm{cm}^{-2} \cdot 30959.14 \cdot 10^{9}\,\mathrm{cm}^{-3}\mathrm{N} \cdot \mathrm{m}^{-1}$$
$$= 313.46 \cdot 10^{-3}\,\mathrm{N} \cdot \mathrm{m}^{-1}$$

which is a rather significant amount. In fact, more accurate estimations should take into account the energy of orientation disclinations, which is a matter for separate study. Just for reference, let us note however, that in the situation of almost complete wetting (with wetting angle $\theta \to 0$) the typical interfacial free energy per unit area, e.g., for the water wetting on the TiO_2 surface, is $\gamma_{LV} \approx 73 \cdot 10^{-3}\,\mathrm{N} \cdot \mathrm{m}^{-1}$, while we have the value $\gamma_{LV} \approx 485 \cdot 10^{-3}\,\mathrm{N} \cdot \mathrm{m}^{-1}$ for the wetting angle θ between 122–140° (which is almost an un-wetting state) of the mercury droplets on the surface of TiO_2[22]. Thus, in our case, the additional energy, generated by the anisotropic character of the wetting liquid as well as of the surface (to be wetted), is quite significant, which may explain the "prohibited" capillary movement of the LC in the laser exposed areas.

Conclusions

The reported study shows that the propagation (due to capillarity) and wetting conditions are dramatically changed as a result of the internal surfaces of substrates (composing the LC cell) being exposed to circularly polarized light. We believe that this phenomenon is related to the orientation of molecules of the solid surface, which reduces the wetting but also which forces the corresponding reorientation of the LC director. The additional energy, related to the director's deformation, changes the balance of forces and the corresponding capillary action. We believe thus that this additional source of energy must be taken into account to correctly describe the capillarity and wetting process and that this phenomenon may have significant fundamental and practical importance. Particularly interesting should be the analysis of the possible impact of this anisotropic mechanism of capillarity in biological systems where an abundant presence of anisotropic liquid structures is reported (cell membranes, fibrils, DNA, collagen structures, etc.) playing crucial roles in living organisms [23].

Acknowledgments

We would like to thank Dr. E. Brasselet for valuable discussions. We would like also to acknowledge the financial support of NSERC Canada.

References

[1] Adamson, A. W., & Gast, A. P. (1997). *Physical Chemistry of Surfaces*, Wiley: New York.
[2] Chaudhury, M. K., & Whitesides, G. M. (1992). *Science*, *256*, 1539.
[3] Fürstner, R., *et al*. (2005). *Langmuir*, *21*, 956.
[4] Cazabat, A. M., *et al*. (1990). *Nature*, *346*, 824.
[5] Schneemilch, M., *et al*. (2000). *Langmuir*, *16*, 2924.
[6] Blake, T. D., Clarke, A., & Stattersfield, E. H. (2000). *Langmuir*, *16*, 2928.
[7] Shin, J. Y., & Abbott, N. L. (1999). *Langmuir*, *15*, 4404.
[8] Ichimura, K., Oh, S.-K., & Nakagawa, M. (2000). *Science*, *288*, 1624.
[9] Sekkat, Z., *et al*. (1994). *Optics Communications*, *111*, 324.
[10] Dumont, D., *et al*. (2002). *Mol. Cryst.&Liq. Cryst.*, *375*, 341.
[11] Chigrinov, V., Kozenkov, V., & Kwok, H.-S. (2008). *Photoalignment of Liquid Crystalline Materials*, Wiley.
[12] de Gennes, P. G., & Prost, J. (1995). *The Physics of Liquid Crystals, Second Edition*, Oxford University Press.
[13] Goubert, G., & Galstian, T. (2009). *Optics Express*, *17*, 9637.
[14] Pham, V. P., *et al*. (1997). *Jpn. Journal of Applied Physics*, *36*, special issue, Part 1, No. 1B, 429.
[15] Yavrian, A., Galstian, T. V., & Piché, M. (2002). *Optical Engineering*, *41*, 852.
[16] Meng, X., *et al*. (1996). *Macromolecules*, *29*, 946.
[17] Yavrian, A., Galstian, T. V., & Piché, M. (2004). *Journal of Optical Materials*, *26*, 261.
[18] Tong, X., Wang, G., & Zhao, Y. (2006). *J. Am. Chem. Soc.*, *128*, 8746.
[19] Grelet, E., & Bock, H. (2006). *Europhys. Lett.*, *73*(5), 712.
[20] Katona, T. T., & Buka, A. (2003). *Physical Review E*, *67*, 041717.
[21] Blinov, L. M., & Chigrinov, V. G. (1994). *Electrooptic Effects in Liquid Crystal Materials*, Springer.
[22] Kataoka, S., & Anderson, M. A. (2004). *Thin Solid Films*, *446*, 232.
[23] Belamie, E., *et al*. (2006). *Journal of Physics: Condens. Matter*, *18*, 115.